Hindawi
Journal of Nanomaterials
Volume 2022, Article ID 6765227, 9 pages
https://doi.org/10.1155/2022/6765227

Research Article

Bioconjugation of Fluorescent Gold Nanoparticles Synthesized Using Marine Brown Algae *Sargassum longifolium*

S. Rajeshkumar,[1] **Hanen Sellami**,[2] **Daoud Ali**,[3] **S. Chitra**,[4] **M. Ponnanikajamideen**,[5] **and Kalirajan Arunachalam**[6]

[1]*Center for Transdisciplinary Research (CFTR), Nanobiomedicine Lab, Department of Pharmacology, Saveetha Dental College, Saveetha Institute of Medical and Technical Science, Saveetha University, Chennai, India*
[2]*Laboratory of Treatment and Valorization of Water Rejects (LTVRH), Water Research and Technologies Center (CERTE), Borj-Cedria Technopark, University of Carthage, Soliman 8020, Tunisia*
[3]*Department of Zoology, College of Science, King Saud University, P. O. Box 2455, Riyadh 11451, Saudi Arabia*
[4]*Department of Prosthodontics, Saveetha Dental College and Hospitals, Saveetha Institute of Medical and Technical Sciences (SIMATS), Chennai 600 077, India*
[5]*Department of Pharmacology and Toxicology, University of Mississippi Medical Centre, Jackson, Mississippi, USA*
[6]*Department of Science and Mathematics, School of Science, Engineering and Technology, Mulungushi University, Kabwe 80415, Zambia*

Correspondence should be addressed to Kalirajan Arunachalam; akalirajan@mu.edu.zm

Received 13 May 2022; Revised 3 June 2022; Accepted 1 July 2022; Published 21 July 2022

Academic Editor: Lakshmipathy R

In the present study, fluorescent gold nanoparticles (Flu Au-NPs) were synthesized via simple and ecofriendly green route using extract of brown algae *Sargassum longifolium* (*S. longifolium*). Characterization of synthesized Au-NPs was undertaken. The characteristic absorption peak of Au-NPs was in range 530 nm in UV-vis spectrum. Scanning electron microscopy (SEM) and transmission electron microscopy (TEM) allow the visualization of the morphological and structural character of Au-NPs. The mean particle size was calculated to be 17-50 nm. Energy dispersive X-ray spectroscopy analysis (EDAX) confirmed the presence of pure gold in the synthesized Au-NPs. The X-ray diffraction (XRD) pattern showed the face-centered cubic (FCC) nature of Au-NPs. Fourier transform infrared spectrometer (FT-IR) showed the characteristic peaks of different biocomponents in the brown algae *S. longifolium* extract which acted as stabilizing or capping agents of Au-NPs.

1. Introduction

Gold nanoparticles (Au-NPs) has been considered a very important and suitable tool in nanotechnology owing to their easier bioconjugation or surface functionalization, stability, and biocompatibility [1]. Moreover, they have been widely applied in various fields especially in medicine, biomedicine, and biology such as drug delivery application to target cancer cell and immunoassays [2, 3]. However, the identification of intracellular Au-NPs could be only used by transmission electron microscopy (TEM). Cell particles imaging by TEM generally includes a complex of ground work procedures such as cells fixation, staining, and dehydration [4]. Confocal laser scanning microscopy could be applied as an alternative technique which confirmed the detection of labelling biomolecules with fluorophore into the cells. Moreover, Au-NPs could be detected using confocal microscopy whether it was coupled with a fluorescent materials. Fluorescence from organic dye could lead to be quenched by energy transference from Au-NPs [Mei-Hui et al., [5], Theresa et al., [6]. Moreover, the combination of fluorophore and Au in a single NP, which maintain the electrical and optical properties of both, could be useful for interfacing with biological systems, reducing nanotoxicity,

modulating electromagnetic fields, multimodal bioimaging, and contacting nanostructures [4, 7, 8]. Au-NPs and rhodamine 6G dye (Rh 6G) were ones of the important metal NP-dye composite system in which the localized surface plasmon resonance band of Au-NP of 530 nm significantly overlaps with the absorption and emission bands of the dye of 525 nm and 550 nm, respectively. This synergistic interaction between the Au-NPs and the Rh 6G dye has found to be useful for different applications like surface-enhanced Raman scattering [9], detection of environmental pollutant [10], and optical molecular spectroscopic ruler [11].

Au-NPs like other metallic nanoparticles have been synthesized by various approaches such as physical, chemical, and biological methods. In the chemical method, mostly toxic agents have been used as reducing and stabilizing agents for NPs' synthesis [12–14]. Nevertheless, these agents caused undesirable toxic effect especially when applied in biomedicine area [15, 16]. Because on the above-mentioned disadvantages, scientists have focused in biosynthesis of NPs using eco-friendly, nontoxic, and lower-cost agents in the synthesis [17]. In this context, green synthesis was an alternative method that used biological material to prepare NPs and contributed to the association between nanobiotechnology and biocompatible systems [18, 19]. Many naturally biological systems, including bacteria, fungi, plants, and algae, have been employed in the biosynthesis of NPs [19–22]. These biological materials possess different biological entities which conduct as both reducing and capping agents in NP fabrication [23, 24]. Green synthesis of metal NPs by using heterocyclic compounds gained more attention due to their important sources of active phytochemicals which served as bionanofactories [25]. Moreover, synthesis of NPs using algae is easy to handle, with high stability and eliminate cell maintenance [26]. In recent times, several studies have reported the use of algae extract such as *Turbinaria conoides* [27], *Sargassum wightii* [28], *Stoechospermum marginatum* [29], and *Laminaria japonica* [30] in green synthesis of Au-NPs.

Sargassum longifolium (*S. longifolium*), a brown algae, was a member of genus *Sargassum* and family *Sargassaceae*. It was widely distributed along Japan and the coasts of Korea, and it has been used in traditional medicine and as food in China and Korea for a long period. In recent years, different physiological properties, such as anti-inflammatory, antioxidant, anticancer, neuroprotective, hypopigmentation, and hepatoprotective, have been reported from *in vitro* and *in vivo* studies using *S. longifolium* extract. It has been mentioned that *Sargassum* species are rich in major bioactive molecule, like phlorotannins, meroterpenoids, fucoxanthins, and fucosterols which are involved in anti-inflammatory and antioxidant properties. Therefore, in this study, the extract from *S. longifolium* was used as a reducing and capping agent to green synthesize Au-NPs. The green-synthesized Au-NPs were then used for investigation of fluorescence quenching of Rh 6G dye. It was reported that the fluorescence quenching of Rh 6G dye by Au-NPs was a result of the formation of a dye-Au-NPs complex. According to our knowledge, the ability of synthesis Au-NPs utilizing *S. longifolium* extract and in the absence of sodium borohydride ($NaBH_4$) for quenching of Rh 6G dye fluorescence is not reported previously. The quenching fluorescence from the Rh 6G and Au-NPs mixture was recovered in the presence of the bovine serum albumin (BSA) protein as a probe. Over the past several years, gold nanoparticles are gaining enormous attention owing to its physicochemical as well as electrical and optical properties. Natural biotemplates, proteins, peptides, and herbal components play an impactful role in the development of gold nanoparticles; in this direction, synthesis of Au-NPs using marine components is one of the frontiers of research. Florescence is a significant probe for imaging, sensing, and cancer therapeutics; hence, bioconjugated gold nanoparticles may rule the medical society with its peculiar properties [31, 32].

2. Materials and methods

2.1. Chemicals. All the chemicals and reagents used in this study were of analytical grade and were purchased from Sigma-Aldrich. All the experimental work was carried out with the assistance of double-distilled water.

2.2. Sample Collection and Preparation of Aqueous Seaweed Extract. Sargassum longifolium, brown seaweed, was collected from coastal areas of Gulf of Mannar (Tamil Nadu, India, latitude 9.1278° N and longitude 79.4662° E) region during low tide in sterile polythene bags and brought to the laboratory. Collected samples were stored at −10°C, and after manually cleaning, the macroalgae was washed for a few times with distilled water to remove any unwanted debris. The algae were dried in air at room temperature until constant mass was obtained. The algal extract was prepared according to the methodology described by Kumar et al. [33] with slight modifications. Briefly, the air-dried seaweeds were grinded into powder using an ordinary grinder. Ten grams of the grinded algae was mixed with 100 mL of deionized water and boiled at 60°C for 30 min. Then, the boiled extract was filtered through nylon mesh cloth and the collected supernatant was stored at 4°C for nanoparticles synthesis.

2.3. Synthesis of Gold Nanoparticles using Seaweed Extracts of Sargassum longifolium. Synthesis of the gold nanoparticles was performed according to the methodology of Rajeshkumar et al. [7]. Typically, 10 mL of pure algal extract solution was mixed with aqueous solution of 90 mL of 1 mM tetrachloroauric acid ($HAuCl_4$) solution and kept at room temperature under constant magnetic stirring at 200 rpm. A color change of the solution was observed visually and UV-vis spectroscopy at different time points and absorbance in the respective wavelength authenticating the presence of gold nanoparticles.

2.4. Purification and Characterization of Synthesized Gold Nanoparticles. The bioreduction of gold ions (Au^{3+}) in aqueous solution using algae extract was monitored by double beam UV-vis spectrophotometer at different wavelengths from 4000 to 700 nm (Perkin Elmer, Singapore). Green-synthesized gold nanoparticles were purified by distilled water by repeated centrifugation at 10,000 rpm for 15 min, and the purified gold particles were dried in hot air oven and stored for further characterization. The crystal nature

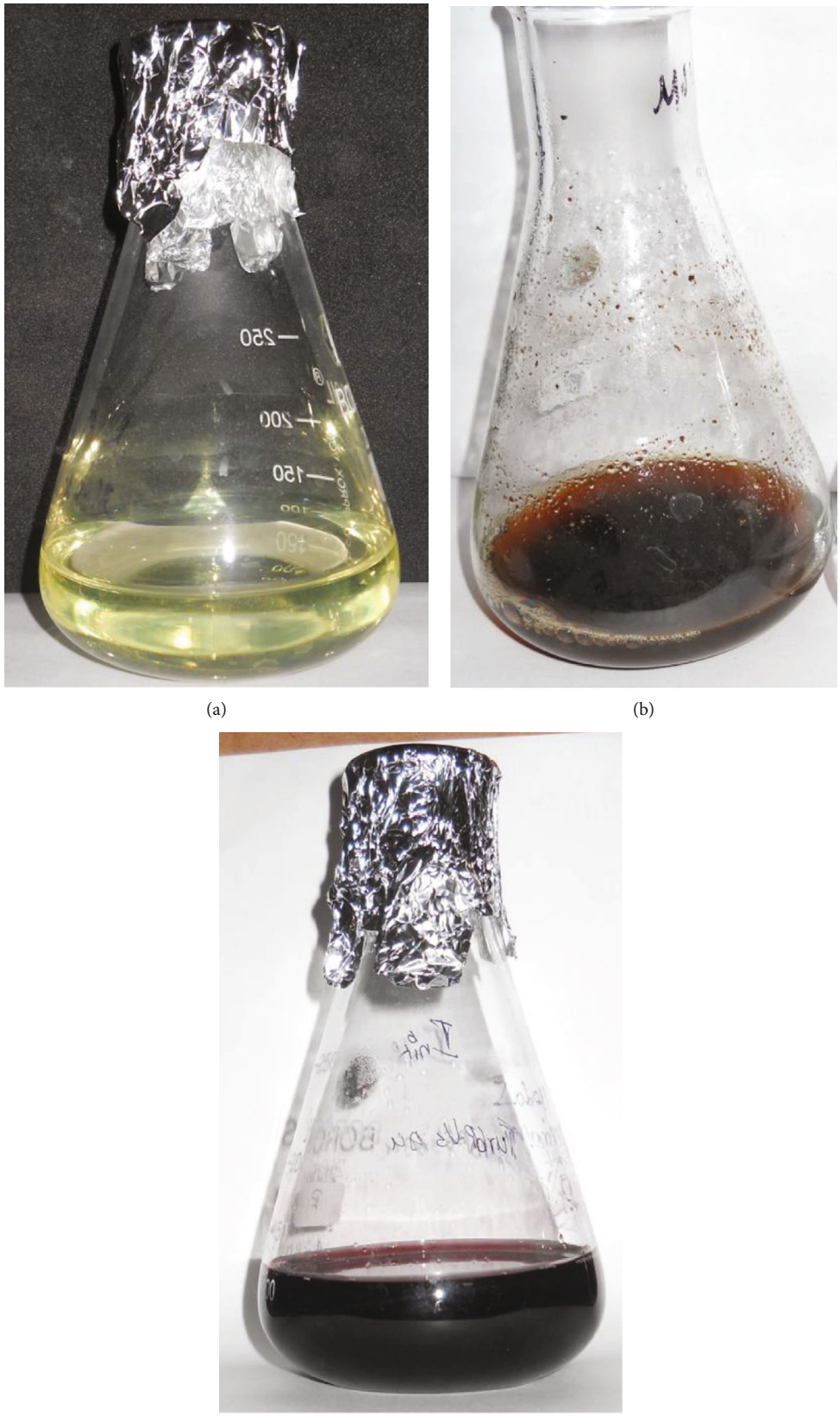

(a) (b)

(c)

Figure 1: Visual observation of Au-NPs synthesis using *S. longifolium* algae extract: (a) 1 mM of gold chloride, (b) algal extract, and (c) synthesized gold nanoparticles.

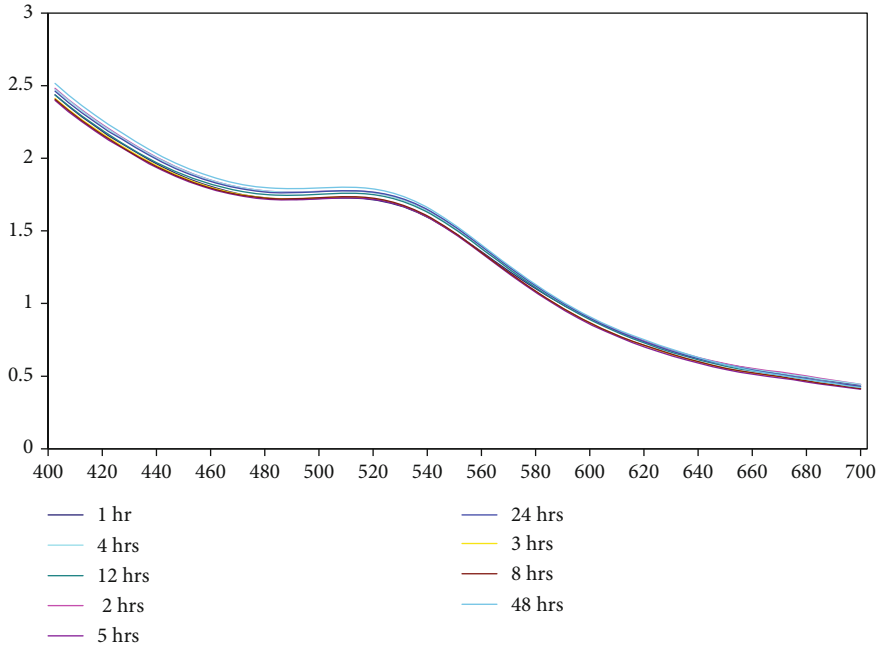

Figure 2: UV-vis spectra recorded the formation of Au-NPs in the reaction mixture of *S. longifolium* algae extract and $HAuCl_4$ at different time intervals showing the peak at 530 nm.

of the purified gold nanoparticles was analyzed by powder X-ray diffractometer (Bruker, Germany; model: D8 Advance). The morphology and particle size distribution were characterized by transmission electron microscope (TEM). The samples for TEM analysis were prepared by drop coating the gold nanoparticle solution on carbon-coated copper grid and leaving them to dry at room temperature. TEM was scanned by a Philips CM 200 model set at an accelerating voltage of 200 kV. The shape and the elemental composition were analyzed by coupling between a scanning electron microscope (SEM) and an energy dispersive X-ray spectroscopy (EDAX) using Philips EDS attached with SEM machine. The functional biomolecules present in the seaweed responsible for the gold nanoparticles formation were characterized by FT-IR (Perkin-Elmer, model 297 IR spectrophotometer). The dried gold nanoparticles were compressed with *KBr* into thin pellets and measured at the wavelength range from 4000 to 400 cm^{-1}.

2.5. Preparation of Fluorescent Gold Nanoparticles. The methodology for the preparation of gold nanoparticles using seaweed extract has been adapted as mentioned previously. Briefly, 5 mL of pure seaweed extract solution was mixed with aqueous solution of 15 mL of 1 mM tetrachloroauric acid ($HAuCl_4$) solution. Then, the solution was kept overnight with constant stirring. The formation of dark pinkish colour indicates the synthesis of gold nanoparticles. For the synthesis of fluorescent gold nanoparticles, 10% of 5 mL rhodamine 6G dye solution was added to the prepared gold nanoparticles solution and kept in magnetic stirrer overnight. After mixing, the reaction mixture was centrifuged at 7500 rpm for 15 min. Afterwards, 0.1 mg of bovine serum albumin (BSA) was added to the solution and stirred overnight. Finally, the mixture was centrifuged at 7500 rpm for 15 min and the obtaining pellet was dried in hot air oven. The formation of fluorescent gold nanoparticles was analyzed by using UV-vis spectroscopy and inverted fluorescent microscope (Leica Microsystems Italia, Milan, Italy).

2.6. Bioconjugation of Antibody with Green-Mediated Fluorescent Gold Nanoparticles. One milliliters of the prepared fluorescent gold nanoparticles was added to 500 μL of BSA solution under the vortex mixing conditions by a vortex mixer. Then, the solution was centrifuged at 7500 rpm for 15 min. After that, from the collected pellet, 100 μL of fluorescent gold nanoparticles were taken and 10 μL of antibody was added from the kit, and the mixture was incubated for overnight at an incubated shaker. After incubation, the conjugated antibody with green-mediated fluorescent gold nanoparticle was viewed using a Leica fluorescence microscope (Leica Microsystems Italia, Milan, Italy).

3. Results and Discussion

3.1. Visual Identification. Reduction of gold ions to Au-NPs was visually identified by color change from 1 h to pinkish red in the aqueous solution of reaction mixture within 10 min of incubation time (Figure 1). The appearance of pinkish red color was due to the excitation of surface plasmon vibrations (SPRs), typical of Au-NPs [28]. The color change depended on the incubation time. The deep pinkish red color for Au-NPs was attained at 24 h indicating that the color intensity was gradually increased when the increased time of incubation. Furthermore, the Au-NPs' formation by the algae extract was confirmed using UV-vis spectroscopy at different wavelengths.

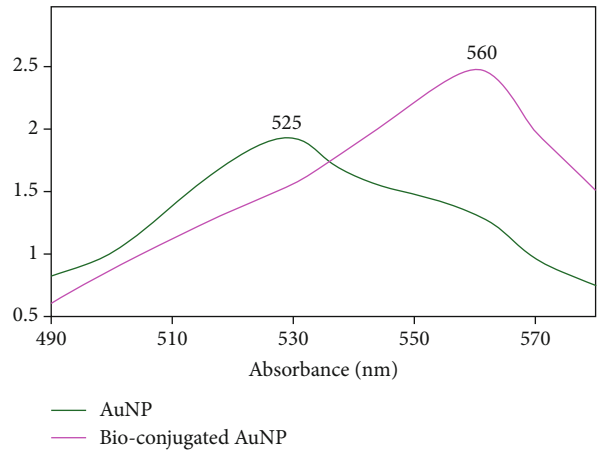

Figure 3: UV-vis spectra of synthesized Au-NPs and bioconjugated Au-NPs.

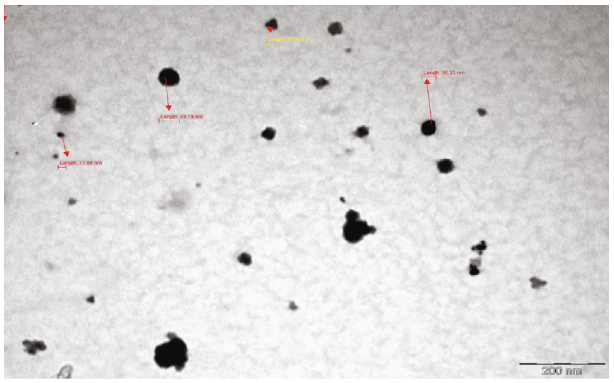

Figure 4: TEM images of Au-NPs synthesized using *S. longifolium* algae extract at 200 nm scale bar showing spherical-shaped nanoparticles.

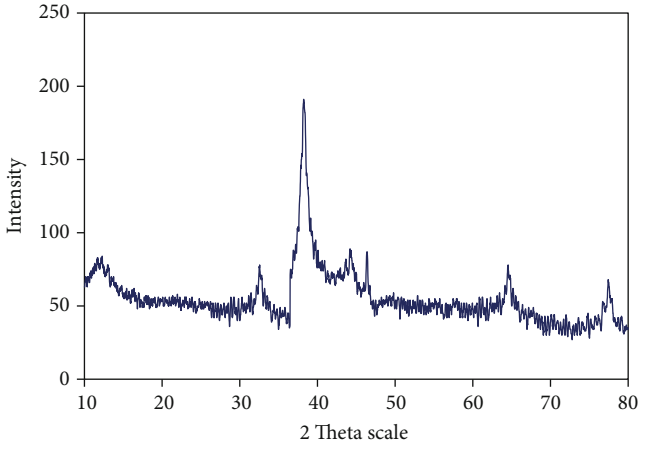

Figure 5: XRD spectra of Au-NPs synthesized using *S. longifolium* algae extract.

3.2. UV-Vis Spectroscopic Analysis. Figure 2 shows the UV-vis spectra of the reaction mixture of gold chloride solution with *S. longifolium* extract that was exposed with different time intervals such as 1 h, 2 h, 3 h, 4 h, 5 h, 8 h, 12 h, 24 h, and 48 h. Herein, the peak was observed at 530 nm which indicates the presence of Au-NPs, which was synthesized by *S. longifolium* algae extract. The peak was raised due to the consequence of SPR [28]. All the peaks were nearly in the first hour peak denotes that after the first hour, the reaction rate was slowly decreased and most of the reaction of nanoparticles synthesis was completed within one hour. After 24 h, the peak was decreased indicating that there is no reaction in the mixture. Figure 3 explicates the absorption spectra of gold nanoparticles and bioconjugated nanoparticles. Generally, absorbance varies with respect to size in the case of gold nanoparticles [34]. The intensity of peaks observed in UV-vis plot remains the same for all time intervals clearly indicating the stability of the gold nanoparticles synthesized using marine brown algae. Surface plasmon absorption indicates the particulate nature; here, λ_{max} is increased in bioconjugated gold nanoparticle (560 nm) than that of the host material (Au-NPs 525 nm), which indicates the enhanced particle growth of bioconjugated gold nanoparticles [35].

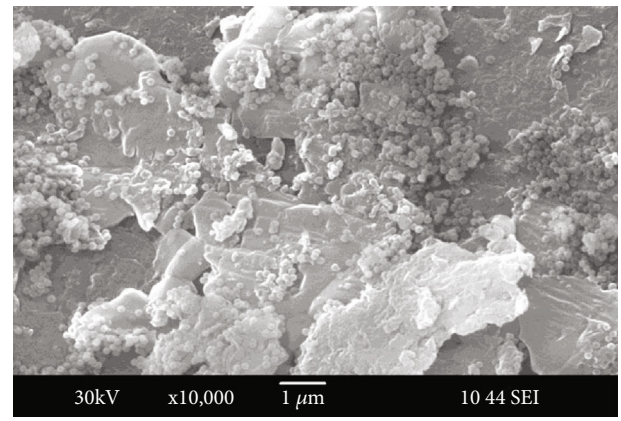

Figure 6: SEM images of Au-NPs synthesized using *S. longifolium* algae extract.

3.3. TEM Analysis. The TEM analysis was performed to identify the morphology of synthesized Au-NPs by algae extract. TEM images indicated the formation of monodispersed-spherical shaped Au-NPs with an average size of nearly 17-50 nm (Figure 4). In this study, the formation of monodispersed nanoparticles was dependent on the presence of biochemicals in the green materials used for the synthesis of Au-NPs [36, 37].

3.4. XRD Analysis. The XRD spectra was used for the confirmation of crystalline nature of the Au-NPs synthesized by using marine brown algae extract, and the pattern is exhibited in Figure 5. The spectrum of XRD clearly indicated that the synthesized Au-NPs are crystalline in nature. The Bragg reflections of Au-NPs that were observed at 2Θ values of 38.36, 44.13, 64.78, and 77.98 were corresponding to the lattice planes (1 1 1), (2 0 0), (2 2 0), and (3 1 1), respectively, which was indexed for FCC gold. The obtained Bragg peaks were compared with pure crystalline gold standard published by Joint Committee on Powder Diffraction Standards (JCPDS), USA (file no. 04-0784). Additionally some small

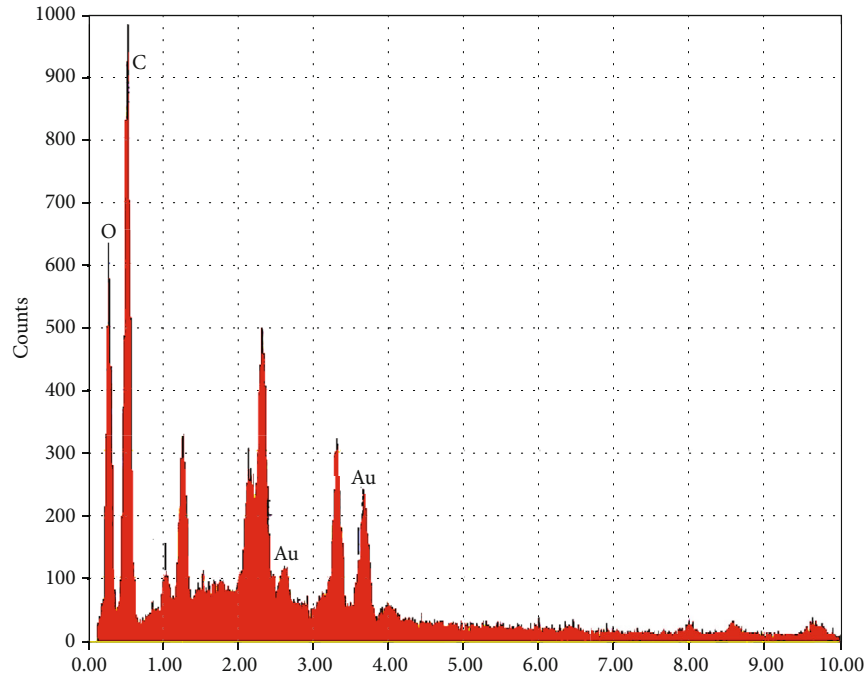

Figure 7: EDAX analysis of *S. longifolium* algae extract-assisted synthesis of Au-NPs.

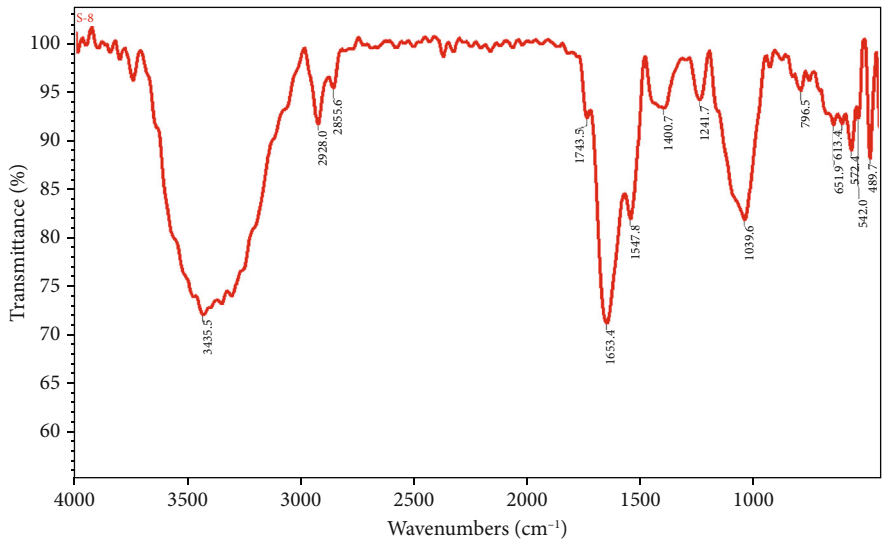

Figure 8: FTIR spectra of *S. longifolium* algae extract-synthesized Au-NPs.

amorphous peaks were present in the spectra that may be due to less biochemicals of the stabilizing agent which were enzymes or proteins in the marine brown algae *S. longifolium* extract. This result was in agreement with the previous report of Rajathi et al. [29] and Rajeshkumar et al. [19] that used brown algae *Stoechospermum marginatum* and *Turbinaria conoides*, respectively, for Au-NPs biosynthesized.

3.5. SEM Analysis. Scanning electron microscope (SEM) was one of the significant tools to identify the shape of the nanoparticles. The structure of the synthesized Au-NPs was exhibited in Figure 6. The Au-NPs synthesized by the marine brown algae *S. longifolium* extract were predominantly spherical in shape. Figure 6 shows also the aggregation of the particles and form a bulk-like structures. This aggregation of nanoparticles was acquired because of the biomolecules of algae, and in the nanoparticles background, some large sized undefined shaped structures found to be a biomolecules attached with the nanoparticles. This report was well matched with the report of UV-vis spectra. In *S. longifolium* algae extract, the reduction of gold metal ions in to Au-NPs was obtained from 30 min to 1 hr. After 1 hr, the growth of nanoparticles was not developed that much in terms of size and the same spherical shaped Au-NPs [38].

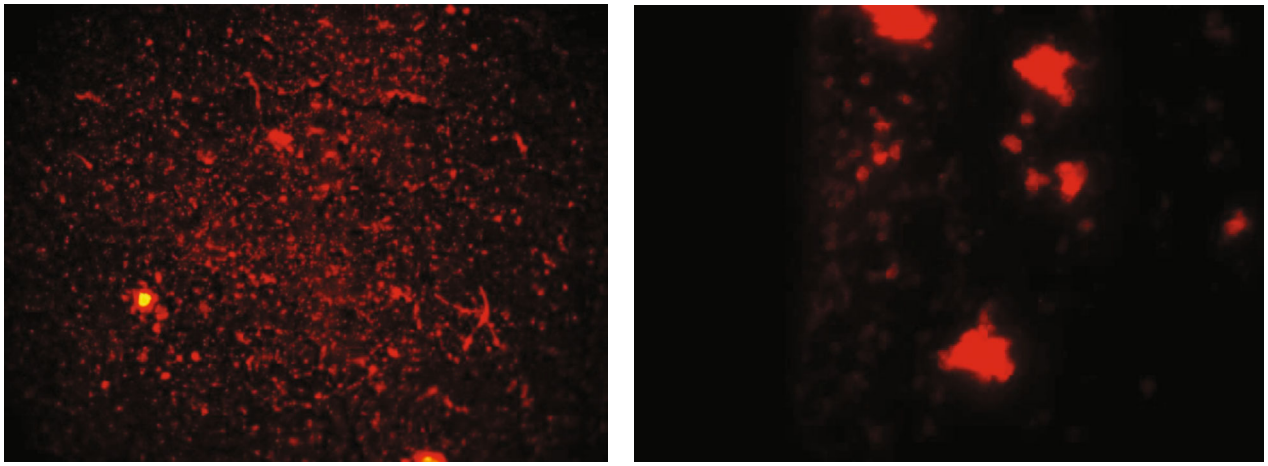

(a) Flu Au-NPs (b) Bioconjugated Au-NPs

Figure 9: Fluorescent microscopic image of gold nanoparticles.

3.6. EDAX Analysis. EDAX analysis was carried out to detect and quantify the elemental composition in the reaction mixture that can be involved in the synthesis of Au-NPs. Figure 7 shows an intense signal at 3 keV which is typical for the absorption of metallic Au-NPs due to surface plasmon resonance. EDAX is authenticating the material formation by exhibiting the presence of Au, O, and C elements. The other peaks present in the EDX spectrum show the metals of and ingredients of marine brown seaweed used to synthesize gold nanoparticles synthesis. The presence of strong signals X-rays to exhibit the presence of gold nanoparticles was quantified through energy-dispersive X-ray spectroscopy.

3.7. FTIR Analysis. FTIR measurement was performed to identify the functional biomolecules in the *S. longifolium* extract responsible for the reduction of gold ions and the stabilization of the synthesized Au-NPs. FTIR spectra ensured functional groups of *S. longifolium* extract involved in the biosynthesized Au-NPs (Figure 8). The band observed at 3,435 cm^{-1} corresponded to the presence of O-H bond stretching in polyphenol and alcohols [39], the absorption band at 2,928 cm^{-1} was attributed to C-H stretching vibrations of the alkanes group, the band at 1,653 cm^{-1} indicates the presence of amide I, the band at 1,400 cm^{-1} corresponded to C-C stretching aromatic rings, the band at 1,241 cm^{-1} corresponded to C-O stretching carboxylic acid group, the peak at 1,039 cm^{-1} was due to the presence of C-N stretching vibration of aliphatic amine of proteins [40], and 796 cm^{-1} was assigned to S-O stretching of sulfonates. The weak bands at 651 and 572 cm^{-1} correspond to alkyl halides. This result confirms that the carbonyl group from proteins or amino acids has high ability to bind metal thus the enzymes or proteins could be mostly possible to cap the metal NPs. This suggestion reveals that amide linkage protein molecules and sulfonated polysaccharide compound could possibly be engaged in the reduction of gold ions to NPs and the stabilization of Au-NPs in the medium.

Gold nanoparticle is one of the unique materials which exhibit fluorescence behavior [41]; plasmonic property of these nanoparticulates gained significant attention owing to the signal amplification at specific frequency [42]. Here, Au-NPs showing fluorescence behavior, after conjugation with biomolecule the fluorescence, were rapidly enhanced which can be visible through the images (Figure 3 and Figures 9(a) and 9(b)). Brightness of sports was tremendously improved in bioconjugated nanoparticles; therefore, it can be understood that excitation and emission are mainly dependent on bandgap and the size distribution of the materials. Biomolecule-tagged nanoparticles may possess emission at higher wavelength as a result of fluorescence; these results have correlation with UV-vis absorption spectra.

4. Conclusion

Gold nanoparticles are majorly used in biomedical applications especially in the imaging, drug delivery, and diagnostics such as cancer detection, and microbial detection. In this study, we clearly explained the bioconjugation of gold nanoparticles to fluorescent gold nanoparticles. UV-vis spectra authenticate the presence of Au-NPs by exhibiting absorption at around 520 nm to 560 nm. The X-ray diffraction results clearly shows the functional group vibration confirms the gold nanoparticles. Spherical nanoparticles with relevant elemental compositions were observed from SEM and EDS. Similarly, fluorescent behavior of gold nanoparticles was noted through fluorescence microscopic images. Preparation of fluorescent gold nanoparticles may upregulate the properties of cancer cell detection; our intention is to develop this material as a diagnostic vehicle to identify cancer.

Data Availability

The research data used to support the findings of this study are included in the article.

Conflicts of Interest

The authors declared no conflict of interest.

Acknowledgments

The authors would like to thank Saveetha Dental College and Hospital, SIMATS, for encouragement. This work was funded by Researchers Supporting Project number RSP-2021/165, King Saud University, Riyadh, Saudi Arabia.

References

[1] A. A. Abdellatif, S. A. El Rasoul, and S. Osman, "Gold nanoparticles decorated with octreotide for somatostatin receptors targeting," *International Journal of Pharmaceutical Sciences and Research*, vol. 7, pp. 14–20, 2015.

[2] K. J. Huang, J. Li, Y. M. Liu, X. Y. Cao, S. Yu, and M. Yu, "Disposable immunoassay for hepatitis B surface antigen based on a graphene paste electrode functionalized with gold nanoparticles and a nafion-cysteine conjugate," *Microchimica Acta*, vol. 177, no. 3-4, pp. 419–426, 2012.

[3] M. Saleh, H. Soliman, O. Haenen, and M. El-Matbouli, "Antibody-coated gold nanoparticles immunoassay for direct detection of Aeromonas salmonicida in fish tissues," *Journal of Fish Diseases*, vol. 34, no. 11, pp. 845–852, 2011.

[4] Q. Wu, L. Chen, L. Huang et al., "Quantum dots decorated gold nanorod as fluorescent-plasmonic dual-modal contrasts agent for cancer imaging," *Biosensors & Bioelectronics*, vol. 74, pp. 16–23, 2015.

[5] M.-H. Tseng, C.-C. Hu, and T.-C. Chiu, "A fluorescence turn-on probe for sensing thiodicarb using rhodamine B functionalized gold nanoparticles," *Dyes and Pigments*, vol. 171, p. 107674, 2019.

[6] T. F. Calangian, Maria, B. Ildefonzo et al., "Facile synthesis of biologically derived fluorescent carbon nanoparticles (FCNPs) from an abundant marine alga and its biological activities," *Oriental Journal of Chemistry*, vol. 34, no. 2, pp. 791–799, 2018.

[7] R. Lakshmipathy, M. K. Kesarla, A. R. Nimmala et al., "ZnS nanoparticles capped with watermelon rind extract and their potential application in dye degradation," *Research on Chemical Intermediates*, vol. 43, no. 3, pp. 1329–1339, 2017.

[8] E. G. Tamil, G. L. Balaji, H. Padhy, and R. Lakshmipathy, "Synthesis of silver nanoplates using regenerated watermelon rind and their application," *Materials Today: Proceedings*, vol. 55, pp. 240–245, 2022.

[9] M. V. Rigo, J. Seo, W. Kim, and S. Jung, "Plasmon coupling of R6G-linked gold nanoparticle assemblies for surface-enhanced Raman spectroscopy," *Vibrational Spectroscopy*, vol. 57, no. 2, pp. 315–318, 2011.

[10] H. Y. Chang, T. M. Hsiung, Y. F. Huang, and C. C. Huang, "Using rhodamine 6G-modified gold nanoparticles to detect organic mercury species in highly saline solutions," *Environmental Science & Technology*, vol. 45, no. 4, pp. 1534–1539, 2011.

[11] T. Sen, S. Sadhu, and A. Patra, "Surface energy transfer from rhodamine 6G to gold nanoparticles: a spectroscopic ruler," *Applied Physics Letters*, vol. 91, 2007.

[12] R. Javed, M. Zia, S. Naz, S. O. Aisida, N. u. Ain, and Q. Ao, "Role of capping agents in the application of nanoparticles in biomedicine and environmental remediation: recent trends and future prospects," *Journal of Nanobiotechnology*, vol. 18, no. 1, p. 172, 2020.

[13] S. Jayakodi, R. Shanmugam, B. O. Almutairi et al., "*Azadirachta indica*- wrapped copper oxide nanoparticles as a novel functional material in cardiomyocyte cells: An ecotoxicity assessment on the embryonic development of *Danio rerio*," *Environmental Research*, vol. 212, article 113153, Part A, 2022.

[14] J. Jose, K. V. Teja, K. Janani et al., "Preparation of a novel nanocomposite and its antibacterial effectiveness against enterococcus faecalis—an in vitro evaluation," *Polymers*, vol. 14, no. 8, p. 1499, 2022.

[15] R. Herizchi, E. Abbasi, M. Milani, and A. Akbarzadeh, "Current methods for synthesis of gold nanoparticles," *Artificial Cells, Nanomedicine, and Biotechnology*, vol. 44, no. 2, pp. 596–602, 2016.

[16] I. Khan, K. Saeed, and I. Khan, "Nanoparticles: properties, applications and toxicities," *Arabian Journal of Chemistry*, vol. 12, no. 7, pp. 908–931, 2019.

[17] V. V. Makarov, A. J. Love, O. V. Sinitsyna et al., ""Green" nanotechnologies: synthesis of metal nanoparticles using plants," *Acta Naturae*, vol. 6, no. 1, pp. 35–44, 2014.

[18] K. Kalimuthu, B. C. Lubin, A. Bazylevich et al., "Gold nanoparticles stabilize peptide-drug-conjugates for sustained targeted drug delivery to cancer cells," *Journal of Nanobiotechnology*, vol. 16, no. 1, p. 34, 2018.

[19] S. Rajeshkumar, C. Malarkodi, G. Gnanajobitha et al., "Seaweed mediated synthesis of gold nanoparticles using *Turbinaria conoides* and its characterization," *Journal of Nanostructure in Chemistry*, vol. 3, no. 1, p. 44, 2013.

[20] R. A. B. Alvarez, M. Cortez-Valadez, L. O. Neira Bueno et al., "Vibrational properties of gold nanoparticles obtained by green synthesis," *Physica E: Low-dimensional Systems and Nanostructures*, vol. 84, pp. 191–195, 2016.

[21] N. Saifuddin, C. W. Wong, and A. A. Nur Yasumira, "Rapid biosynthesis of silver nanoparticles using culture supernatant of bacteria with microwave irradiation," *Journal of Chemistry*, vol. 6, no. 1, 2009.

[22] K. Vahabi, G. A. Mansoori, and S. Karimi, "Biosynthesis of silver nanoparticles by fungus Trichoderma Reesei (a route for large-scale production of AgNPs)," *Insciences Journal*, vol. 1, pp. 65–79, 2011.

[23] S. Iravani, "Green synthesis of metal nanoparticles using plants," *Green Chemistry*, vol. 13, no. 10, pp. 2638–2650, 2011.

[24] S. Viswanathan, T. Palaniyandi, P. Kannaki et al., "Biogenic synthesis of gold nanoparticles using red seaweed Champia parvula and its anti-oxidant and anticarcinogenic activity on lung cancer," *Particulate Science and Technology*, pp. 1–9, 2022.

[25] V. Patel, D. Berthold, P. Puranik, and M. Gantar, "Screening of cyanobacteria and microalgae for their ability to synthesize silver nanoparticles with antibacterial activity," *Biotechnology Reports*, vol. 5, pp. 112–119, 2015.

[26] S. Rajeshkumar, C. Kannan, and G. Annadurai, "Green synthesis of silver nanoparticles using marine brown algae *Turbinaria conoides* and its antibacterial activity," *International Journal of Pharma and Bio Sciences*, vol. 3, pp. 502–510, 2012.

[27] K. Vijayaraghavan, A. Mahadevan, M. Sathishkumar, S. Pavagadhi, and R. Balasubramanian, "Biosynthesis of Au(0) from Au(III) via biosorption and bioreduction using brown marine alga *Turbinaria conoides*," *Chemical Engineering Journal*, vol. 167, no. 1, pp. 223–227, 2011.

[28] G. Singaravelu, J. S. Arockiamary, K. V. Ganesh, and K. Govindaraju, "A novel extracellular synthesis of monodisperse gold nanoparticles using marine alga, *Sargassum wightii* Greville," *Colloids and Surfaces B: Biointerfaces*, vol. 57, no. 1, pp. 97–101, 2007.

[29] F. A. A. Rajathi, C. Parthiban, V. Ganesh Kumar, and P. Anantharaman, "Biosynthesis of antibacterial gold nanoparticles using brown alga, *Stoechospermum marginatum* (kützing)," *Spectrochimica Acta Part A: Molecular and Biomolecular Spectroscopy*, vol. 99, pp. 166–173, 2012.

[30] G. Ghodake and D. S. Lee, "Biological synthesis of gold nanoparticles using the aqueous extract of the brown *algae Laminaria japonica*," *Journal of Nanoelectronics and Optoelectronics*, vol. 6, no. 3, pp. 268–271, 2011.

[31] N. Kaur, R. N. Aditya, A. Singh, and T.-R. Kuo, "Biomedical applications for gold nanoclusters: recent developments and future perspectives," *Nanoscale Research Letters*, vol. 13, no. 1, p. 302, 2018.

[32] D. O. Plaza, C. Gallardo, Y. D. Straub, D. Bravo, and J. M. Pérez-Donoso, "Biological synthesis of fluorescent nanoparticles by cadmium and tellurite resistant Antarctic bacteria: exploring novel natural nanofactories," *Microbial Cell Factories*, vol. 15, no. 1, p. 76, 2016.

[33] P. Kumar, S. S. Selvi, A. L. Prabha, K. P. Kumar, R. S. Ganeshkumar, and M. Govindaraju, "Synthesis of silver nanoparticles from *Sargassum tenerrimum* and screening phytochemicals for its antibacterial activity," *Nano-Biomedical Engineering*, vol. 4, no. 1, pp. 12–16, 2012.

[34] Stephan and M. A. El-Sayed, "Size and temperature dependence of the plasmon absorption of colloidal gold nanoparticles," *Temperature Dependence of the Plasmon Absorption of Colloidal Gold Nanoparticles.*, vol. 103, no. 21, pp. 4212–4217, 1999.

[35] W. Haiss, N. T. K. Thanh, J. Aveyard, and D. G. Fernig, "Determination of size and concentration of gold nanoparticles from UV−vis spectra," vol. 79, no. 11, pp. 4215–4221, 2007.

[36] D. Philip, "Green synthesis of gold and silver nanoparticles using *Hibiscus rosa sinensis*," *Physica E: Low-dimensional Systems and Nanostructures*, vol. 42, no. 5, pp. 1417–1424, 2010.

[37] S. L. Smitha, D. Philip, and K. G. Gopchandran, "Green synthesis of gold nanoparticles using *Cinnamomum zeylanicum* leaf broth," *Spectrochimica Acta Part A: Molecular and Biomolecular Spectroscopy*, vol. 74, no. 3, pp. 735–739, 2009.

[38] S. Rajeshkumar, M. Vanaja, and A. Kalirajan, "Degradation of toxic dye using phytomediated copper nanoparticles and its free-radical scavenging potential and antimicrobial activity against environmental pathogens," *Bioinorganic Chemistry and Applications*, vol. 2021, Article ID 1222908, 10 pages, 2021.

[39] J. S. Devi, A. Bhimb, and B. V. Ratnam, "*In vitro* anticancer activity of silver nanoparticles synthesized using the extract of *Gelidiella* sp," *International Journal of Pharmacy and Pharmaceutical Sciences*, vol. 4, pp. 710–715, 2012.

[40] A. Gole, C. Dash, V. Ramakrishnan et al., "Pepsin-gold colloid conjugates: preparation, characterization and enzymatic activity," *Langmuir*, vol. 17, no. 5, pp. 1674–1679, 2001.

[41] A. Silvestri, D. Di Silvio, I. Llarena et al., "Influence of surface coating on the intracellular behaviour of gold nanoparticles: a fluorescence correlation spectroscopy study," *Nanoscale*, vol. 9, no. 38, pp. 14730–14739, 2017.

[42] D. S. Reis, V. L. de Oliveira, M. L. Silva, R. M. Paniago, L. O. Ladeira, and L. M. Andrade, "Gold nanoparticles enhance fluorescence signals by flow cytometry at low antibody concentrations," *Journal of Materials Chemistry B*, vol. 9, no. 5, pp. 1414–1423, 2021.

[43] S. Rajeshkumar, S. Menon, S. Venkat Kumar, M. Ponnanikajamideen, D. Ali, and K. Arunachalam, "Anti-inflammatory and antimicrobial potential of Cissus quadrangularis-assisted copper oxide nanoparticles," *Journal of Nanomaterials*, vol. 2021, Article ID 5742981, 11 pages, 2021.